Chapter 1

NUMERICAL SIMULATIONS OF PARTIALLY PREMIXED TURBULENT COMBUSTION

D.C. Haworth
The Pennsylvania State University, University Park, PA, USA

C. Jiménez, B. Cuenot, T. Poinsot
CERFACS, Toulouse, France

and R.J. Blint
GM R&D Center, Warren, MI, USA

Abstract Turbulent flame propagation through non–homogeneous reactant mixtures is investigated using high–resolution two–dimensional numerical simulation, including detailed chemical kinetics and molecular transport. Systematic variations in the distribution of reactant composition are imposed, and the effect of these variations on the primary propagating flame, secondary post–flame reaction, and pollutant formation are analyzed. In this manner, new fundamental insight into partially premixed turbulent flame propagation is generated and information relevant to modeling practical combustion systems is developed.

Keywords: partially premixed turbulent combustion, combustion simulation

1. Introduction

The propagation of a turbulent flame through a reactant mixture of non–uniform strength (e.g., spatial variations in equivalence ratio) is a problem of immense fundamental interest and practical importance. Interest in partially premixed systems has been motivated by recent trends in practical combustion systems. Automotive manufacturers have been moving towards increasingly stratified combustion systems such as direct–injection spark–ignition gasoline engines (Zhao, Lai and Harrington, 1999) to reduce fuel consumption. At the same time, gas–turbine manufacturers have been moving towards increasing levels of premixing to reduce NO_x emissions (Lefebvre, 1998). Significant gaps in fundamental physical understanding of flame propagation, combustion stability, and pollutant formation have kept these systems from achieving their full potential.

Here a simulation–based approach is used to address these issues. The objectives are to generate new fundamental physical understanding of turbulent combustion with non–homogeneous reactants, and to develop and validate turbulent combustion models suitable for device–scale engineering computations (CFD) of practical combustion systems.

2. Partially Premixed Flame Propagation

A two–stage combustion process is hypothesized (Haworth et al., 2000). A healthy essentially premixed flame (established by spark discharge, in the case of a gasoline direct–injection engine) propagates into a stratified reactant mixture; this flame is responsible for most of the heat release. Behind the flame in locally fuel–lean zones are products of combustion, oxidizer, and active radicals; in locally fuel–rich zones are products, fuel fragments or stable intermediates (CO and H_2), and radicals. Eventually the post–flame reactants mix and complete the reaction in a secondary combustion zone, which also is the site for formation and burnout of key pollutant species such as NO and CO.

Several competing effects determine whether the premixed burn rate is increased or reduced as a result of reactant non–homogeneity (Jiménez et al., 2001). For example, flame area is expected to be higher for non–homogeneous reactants by virtue of increased wrinkling as the flame encounters stronger/weaker reactant pockets, while burn rate per unit flame area may be lower or higher, depending on the distribution of equivalence ratio along the active flame front. Early numerical studies of turbulent flame propagation through globally stoichiometric reactants reported modest differences in the premixed burn rate between homogeneous and non–homogeneous reactants (Hélie and Trouvé, 1998) (Haworth et al., 2000). More recently, large variations in burn rate have been found in simulations with globally fuel–lean reactants (Jiménez et al., 2001).

These computational findings can be contrasted with the experimental measurements of Zhou et al. (1998) for a constant–volume bomb. Measurements were taken over a range of rms turbulence levels u', equivalence ratios ϕ (ϕ = 0.7 to ϕ = 1.6), and degrees of heterogeneity α (α = 0 for a homogeneous mixture). For all equivalence ratios, the burn rate first increased and then decreased with increasing α, the variation being as much as a factor of three. An increase in flame corrugation was noted with increasing α. These results suggest that there is an optimum level of reactant stratification for fastest burn.

Secondary post–flame burning also is of interest. The rate of NO_x formation, for example, is affected by variations in local temperature and radical concentrations. Shih, Lee and Santavicca (1996) reported significant increases in NO and NO_x with incomplete fuel–air mixing at a fuel–lean condition ($\phi = 0.6$) for a gas–turbine combustor configuration, while at a condition closer to stoichiometric ($\phi = 0.92$), NO and NO_x decreased as the level of mixedness decreased.

3. A Model Problem

The system considered is a compressible multi–component reacting ideal–gas mixture. Propane–air oxidation is described using a 28–species 73– reaction scheme (Haworth et al., 2000). In some cases, this has been supplemented with an extended Zeldovich thermal NO mechanism (Jiménez et al., 2001). The governing equations and numerical methodology are described fully in Baum (1994).

The governing equations are solved in a two–dimensional rectangular domain. A steady planar laminar premixed flame initially separates reactants from products. Isotropic two–dimensional turbulence is prescribed using a two–parameter turbulence energy spectrum (Haworth and Poinsot, 1992), where the two parameters correspond to the initial rms turbulence velocity u'_{T0} and integral length scale l_{T0}. A turbulence Reynolds number is defined as $Re_{T0} \equiv \rho_u u'_{T0} l_{T0}/\mu_u$, where subscript u refers to unburned–gas properties. Non–homogeneity is introduced by varying the reactant mass fractions of C_3H_8, O_2, and N_2 in a manner that maintains the same total quantity of fuel and oxidizer as for a baseline homogeneous case, and maintains a uniform ratio of O_2 to N_2 . A stratification scale is defined as $l_{\phi 0} \equiv L_y/n$, where L_y is the y–direction length of the domain (parallel to the initial flame) and n is the number of periods in $Y_{C_3H_8}$ across L_y. Both symmetrical and asymmetrical distributions of $Y_{C_3H_8}$ have been investigated (Table 1.1).

Aero–thermo–chemical conditions approach those in an automotive gasoline direct–injection engine at a low–speed light–load operating condition: $p = 4$ atm, $T_u = 700$ K (unburned gas temperature), $u'_{T0} = 7.7$ m/s, and $l_{T0} = 0.23$ mm. It is the turbulence length scale that is furthest from being typical of a practical engine ($l_T \approx 2$ mm – 4 mm near piston top–dead–center).

A chemical time scale is defined as the time required for the change in reactant stoichiometry to penetrate the primary premixed flame: $\tau_f = 2\delta_l^0/[s_l^0(1 + \rho_u/\rho_b)]$. Here ρ_u and ρ_b are the unburned– and burned–gas

Table 1.1. Simulation parameters.[a]

Case[b]	ϕ_{glob}	$\frac{\tau_f}{\tau_{T0}}$	$\frac{u'_{T0}}{s_l^0}$	$\frac{l_{T0}}{\delta_l^0}$	Re_{T0}	n	ϕ_{min}/ϕ_{max}	$\frac{l_{\phi 0}}{l_{T0}}$	*NO*
H_1.0_23	1.0	1.26	4.67	1.57	71	0	1.0/1.0	∞	no
NH_1.0_23	1.0	1.26	4.67	1.57	71	1	0.5/2.7	20.0	no
H_0.6_33	0.6	7.35	11.6	1.58	105	0	0.6/0.6	∞	yes
NHA_0.6_33	0.6	7.35	11.6	1.58	105	1	0.06/1.14	13.0	yes
NHB_0.6_33	0.6	7.35	11.6	1.58	105	1	0.03/2.06	13.0	yes
NHC_0.6_33	0.6	7.35	11.6	1.58	105	4	0.05/2.06	3.3	yes
H_1.0_43	1.0	0.84	4.67	2.36	105	0	1.0/1.0	∞	no
NHA_1.0_43	1.0	0.84	4.67	2.36	105	1	0.10/1.98	13.0	no
NHB_1.0_43	1.0	0.84	4.67	2.36	105	2	0.10/1.98	6.5	no
NHC_1.0_43	1.0	0.84	4.67	2.36	105	4	0.10/1.98	3.3	no
NHD_1.0_43	1.0	0.84	4.67	2.36	105	8	0.10/1.98	1.6	no
NHE_1.0_43	1.0	0.84	4.67	2.36	105	16	0.10/1.98	0.8	no

[a]Pressure is four atmospheres, reactant temperature is 700 K. [b]The final two numbers in the Case name refer to the size of the computational domain; e.g., *_23* is 2 mm × 3 mm.

mass density, respectively, and δ_l^0 and s_l^0 are the laminar flame thickness and speed for the initial one–dimensional steady unstrained premixed flame. For the present thermo–chemical conditions: $\delta_l^0 = 0.096$ mm, $s_l^0 = 1.65$ m/s for $\phi = 1.0$; and $\delta_l^0 = 0.142$ mm, $s_l^0 = 0.66$ m/s for $\phi = 0.6$.

Two additional quantities characterizing partially premixed combustion are a mixture fraction z and a progress variable c (Haworth et al., 2000). Here the mixture fraction is defined as a carbon–plus–hydrogen element mass fraction; the value of z corresponding to reactants in stoichiometric proportion is $z_{st} = 0.06095$. Equivalence ratio ϕ is related to mixture fraction by $\phi = (z/(1-z)) \cdot ((1-z_{st})/z_{st})$. The reaction progress variable is defined in terms of the mixture fraction: $c = 1 - Y_{C_3H_8}/z$. In unburned reactants, $z = Y_{C_3H_8}$ so that $c = 0$; and at any point where there is no propane, $c = 1$. The secondary reaction zone is distinguished from the primary flame based on c: $c > c^*$, with $c^* = 0.9999$.

4. Results

4.1. The Primary Premixed Flame

The maximum difference in flame length between homogeneous and non–homogeneous reactants for equivalent global mixture strength ϕ_{glob} is less than 20%, while maximum differences in heat release exceed 50%. The largest differences have been for globally fuel–lean reactants having an asymmetrical equivalence ratio distribution. Global heat re-

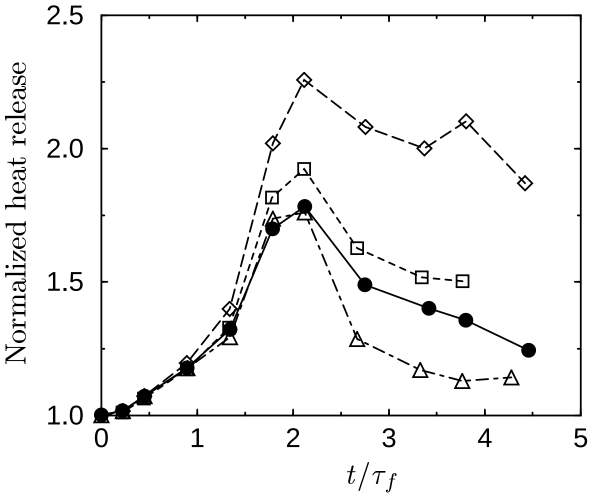

Figure 1.1. Time evolution of total heat release, normalized by its initial value, for globally fuel–lean reactants. Case H_0.6_33 (•) is a homogeneous case, and Cases NHA_0.6_33 (▫), NHB_0.6_33 (⋄), and NHC_0.6_33 (△) have different distributions of reactant non–homogeneities (Table 1.1).

lease for non–homogeneous reactants can be lower or higher than for an equivalent–strength homogeneous mixture (Figure 1.1). These differences result from interactions between turbulence and the propagating flame and the distribution of equivalence ratio along the active flame front (Jiménez et al., 2001).

A quantitative assessment of an engineering combustion model is provided in Figure 1.2. There the computed global heat release is compared to that obtained using a simple flamelet approximation (Jiménez et al., 2001). Following an initial transient, agreement between the simulations and the model is surprisingly good, given the simplicity of the model (neglect of strain, unsteady effects, curvature effects, etc.). This suggests that relatively simple adaptations of laminar flamelet models developed for homogeneous premixed turbulent combustion may suffice to describe the primary heat release in highly non–homogeneous systems.

4.2. Secondary Combustion

Attempts to describe the secondary reaction zone using flamelet concepts have not been successful (Haworth et al., 2000), (Jiménez et al., 2001). Results from a conditional moment closure (CMC) model (Bilger, 1993) have been somewhat more positive. A “first–order” CMC

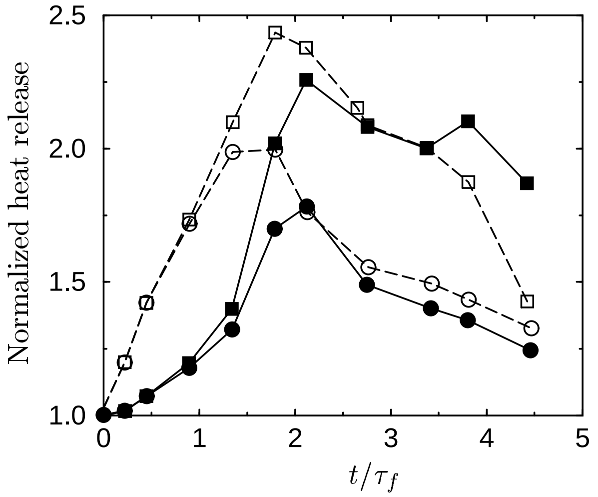

Figure 1.2. Assessment of a premixed flamelet model. Case H_0.6_33 (simulation •, model ∘), homogeneous reactants; Case NHB_0.6_33 (simulation ■ , model □), non–homogeneous reactants.

hypothesis is that the conditional average of the species–α chemical production rate $\dot{\omega}_\alpha$ is equal to the chemical production rate evaluated using the conditionally averaged composition and temperature:

$$\langle \dot{\omega}_\alpha(\underline{Y}, T)|z = \eta\rangle = \dot{\omega}_\alpha(\langle \underline{Y}|z = \eta\rangle, \langle T|z = \eta\rangle) \quad , \tag{1.1}$$

and similarly for heat release. The CMC model is evaluated by comparing the left– and right–hand sides of Eq. 1.1 (Figure 1.3). In general, good agreements is found for heat release, key carbon–containing species (CO, CO_2), and other slow–chemistry–dominated species (e.g., NO); agreement is less satisfactory for radical species and for hydrogen–containing species. The latter discrepancy may be a result of differential diffusion.

4.3. Pollutant Emissions (NO)

Conventional engineering practice in modeling thermal NO production is to neglect reverse reactions (appropriate for low NO concentrations) and to invoke a steady–state approximation for N–atom concentration. Then the local rate of NO formation can be expressed as,

$$\frac{d[\mathrm{NO}]}{dt} = 2k_f[\mathrm{O}][\mathrm{N}_2] \quad , \tag{1.2}$$

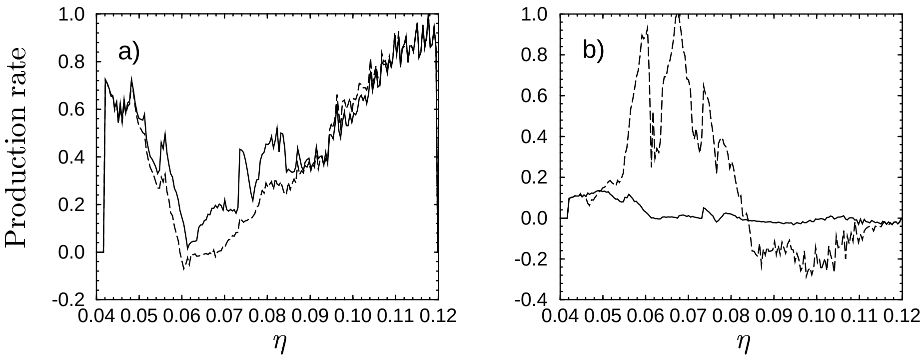

Figure 1.3. Assessment of a CMC model for secondary combustion, Case NH_1.0_23 at $t/\tau_f \approx 3.5$. Solid lines (———) $\langle \dot{\omega}_\alpha(\underline{Y}, T)|z = \eta\rangle$; dashed lines (– – – –) $\dot{\omega}_\alpha(\langle \underline{Y}|z = \eta\rangle, \langle T|z = \eta\rangle)$. The ordinate is normalized by the maximum value for each frame. a) Heat release rate. b) Chemical production rate of OH.

where square brackets indicate molar concentrations and $k_f = k_f(T)$ is the forward rate coefficient for the reaction $O + N_2 \rightleftharpoons NO + N$ (Turns, 2000). Often it is further assumed that the O–atom concentration corresponds to chemical equilibrium. Quantitative assessment of these approximations has been made by comparing results obtained using the full extended Zeldovich mechanism with those obtained using the simplifications (Jiménez et al., 2001). For the conditions simulated, steady–state N–atom and neglect of reverse reactions are quite good approximations, while neglecting superequilibrium O–atom severely underpredicts NO formation. These results pertain only to the initial formation of NO in and immediately behind the primary flame, because of the limited extent of the computational box.

NO formation is found to vary strongly with the length scale of the initial reactant stratification. For the conditions simulated, non–homogeneous reactants yield higher NO levels compared to an equivalent–strength homogeneous mixture. In the case of globally stoichiometric reactants, the total quantity of NO in the computational domain for large–scale non–homogeneities ($n = 1$, $n = 2$) is over 100 times greater than for homogeneous reactants (Figure 1.4). As the length scale of the non–homogeneity decreases (n increases), the homogeneous results are recovered. The high NO levels for non–homogeneous reactants are a consequence of locally high O–atom concentrations and temperatures compared to the homogeneous case (Jiménez et al., 2001). Again, these findings pertain only to the initial formation of NO.

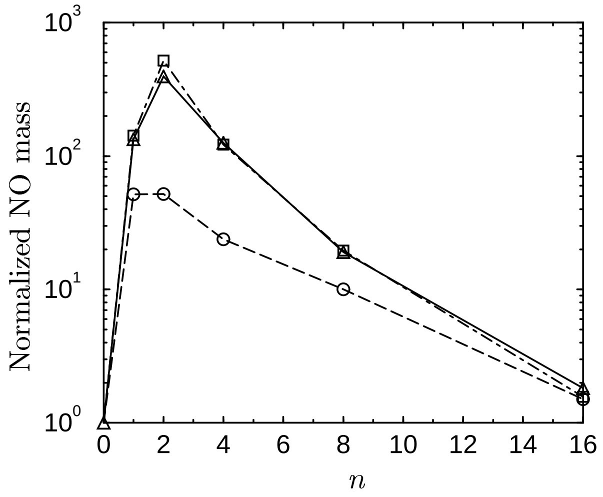

Figure 1.4. NO mass, normalized by that for the homogeneous case ($n = 0$), versus wavenumber of non–homogeneity n at time $t/\tau_f = 4.8$ for globally stoichiometric reactants (cases H_1.0_43 and NHA–E_1.0_43, Table 1.1). Primary flame ($0.5 \leq c \leq 0.9999$) ---- ; secondary combustion zone ($c > 0.9999$) –·– ; total ——— .

4.4. Heat–Release Marker Species

To extract the full potential from modern laser–based combustion diagnostics, it is necessary to correlate measurable quantities (e.g., instantaneous concentrations of single or multiple chemical species) with important but experimentally inaccessible quantities including heat release. Recent suggestions for heat–release/flame markers include the formyl radical (HCO) and simultaneous presence of formaldehyde (CH_2O) and hydroxyl radical (OH) (Najm et al., 1998). Correlations of heat release with mass fractions of several chemical species from the present simulations have served to corroborate and to extend to highly non–homogeneous turbulent flames the marker species proposed in the literature (Haworth et al., 2000).

5. Summary and Conclusions

Numerical simulations provide new insights into several aspects of partially premixed turbulent combustion. Additional results and discussion can be found in Haworth et al. (2000) and Jiménez et al. (2001). Salient findings/results include:

- Heat release and NO can be lower or substantially higher for non–homogeneous reactants compared to an equivalent–strength homogeneous mixture, depending on the nature of the non–homogeneities. This is in qualitative agreement with experimental measurements.
- Relatively small differences in flame length have been found for homogeneous versus non–homogeneous reactants, in apparent contradiction with experiment.
- Steady–state N–atom concentration and neglect of reverse reactions are excellent approximations for modeling the initial thermal NO formation. Equilibrium O–atom is a very poor approximation.
- A simple premixed flamelet model yields generally good results for the primary premixed burn.
- CMC satisfactorily represents heat release, major carbon–containing species, and NO in the secondary reaction zone, while doing less well for hydrogen–containing species and radicals.
- HCO and simultaneous presence of CH_2O and OH correlate nearly linearly with heat release in the primary and secondary combustion zones for homogeneous and non–homogeneous reactants.

The temptation to extrapolate these results to practical combustion systems must be tempered by an awareness of the limitations of the model problem. These include spatial two–dimensionality, neglect of radiation, incomplete chemical kinetics, limited integration times, limited number of realizations for statistical analysis, and the small dynamic range of length scales. In the authors' opinion, it is the last of these that is most restrictive, and which most likely is responsible for the failure to find large differences in flame length. Implications of spatial two–dimensionality are discussed in Haworth and Poinsot (1992).

Acknowledgments

This research was initiated during the 1998 and 2000 Summer Programs of the Stanford University/NASA Ames Center for Turbulence Research. Computational resources have been provided by CTR, the Institut du Développement et des Resources en Informatique Scientifique (IDRIS), and the GM R&D Center.

References

Baum, M. (1994). Etude de l'allumage et de la structure des flames turbulentes. Ph.D. Thesis, Ecole Central, Paris.

Bilger, R. W. (1993). Conditional moment closure for turbulent reacting flow. *Phys. Fluids A.* 5:436–444.

Haworth, D. C., Blint, R. J., Cuenot, B. and Poinsot, T. J. (2000). Numerical simulation of turbulent propane–air combustion with non–homogeneous reactants. *Combust. Flame.* 121:395–417.

Haworth, D. C. and Poinsot, T. J. (1992). Numerical simulations of Lewis number effects in turbulent premixed flames. *J. Fluid Mech.* 244:405–436.

Hélie, J. and Trouvé, A. (1998). Turbulent flame propagation in partially premixed combustion. *Proc. Combust. Institute.* 27:891–898.

Jiménez, C., Haworth, D., Cuenot, B. and Poinsot, T. (2001). Direct numerical simulation and modeling of lean stratified propane–air flames. *Combust. Flame.* To appear.

Lefebvre, A. H. (1998). *Gas Turbine Combustion*, Second Edition. Taylor & Francis.

Najm, H. N., Paul, P. H., Mueller, C. J. and Wyckoff, P. S. (1998). On the adequacy of certain experimental observables as measurements of flame burning rate. *Combust. Flame.* 113:312–332.

Shih, W. P., Lee, J. G. and Santavica, D. A. (1996). Stability and emission characteristics of a lean premixed gas turbine combustor. *Proc. Combust. Institute.* 26:2771–2778.

Turns, S. R. (2000). *An Introduction to Combustion*, Second Edition. McGraw–Hill.

Zhao, F. Q., Lai, M. C. and Harrington, D. L. (1999). Automotive spark–ignited direct–injection gasoline engines. *Prog. Energy Combust. Sci.* 25:437–562.

Zhou, J., Nishida, K., Yoshikazi T. and Hiroyasu, H. (1998). Flame propagation characteristics in a heterogeneous concentration distribution of a fuel–air mixture. *SAE Paper No. 982563.*